# Predicting the mixing time of soft elastic reactors: Physical models and empirical correlations

Xiao Dong Chen, Guillaume Delaplace, Minghui Liu, Romain Jeantet, Jie Xiao

Thermodynamics, Transport, and Fluid Mechanics

# Predicting the mixing time of soft elastic reactors: Physical models and empirical correlations

Guillaume Delaplace, Minghui Liu, Romain Jeantet, Jie Xiao, and Xiao Dong Chen

*Ind. Eng. Chem. Res.*, **Just Accepted Manuscript** • DOI: 10.1021/acs.iecr.9b06053 • Publication Date (Web): 05 Mar 2020

# Predicting the mixing time of soft elastic reactors: Physical models and empirical correlations

Guillaume Delaplace[1,2*], Minghui Liu[3], Romain Jeantet[1,4], Jie Xiao[1,3*], Xiao Dong Chen[1,3]

[1]International Associated Laboratory - FOODPRINT (INRA Villeneuve d'Ascq-Soochow University-Agrocampus Rennes), Soochow University, Suzhou, Jiangsu 215123, China

[2]Unité Matériaux et Transformations (UMET) - UMR 8207, INRA, Team PIHM, 369 rue Jules Guesde, 59651 Villeneuve d'Ascq, France

[3]School of Chemical and Environmental Engineering, College of Chemistry, Chemical Engineering and Materials Science, Soochow University, Suzhou, Jiangsu 215123, China

[4]STLO, UMR 1253, INRA, Agrocampus Ouest, 35000 Rennes, France

*Corresponding authors: Guillaume Delaplace (guillaume.delaplace@inra.fr) and Jie Xiao (jie.xiao@suda.edu.cn)

## Abstract

The aim of this study was to experimentally determine the mixing times of viscous fluids placed in a soft container where they were mixed by the vibrations of the tank wall. In parallel, mechanistic models were established to link the inlet parameters of the crank/slider device responsible for the tank wall vibrations to the mixing times.

The mechanistic models are based on dimensional analysis. Either momentum change (change in instantaneous velocity with which the slider comes in contact with the soft elastic reactor) or impulse (force transmitted by the piston) is introduced as an intermediate parameter in the relevant list of physical quantities in order to take the intensity of mechanical sollicitation induced by the beater into account. These two intermediate parameters were theoretically

computed on the basis of knowledge about the geometrical parameters and the rotational speed of the crank/slider device.

The experimental results showed that the mixing time strongly depends on momentum change (or impulse) induced by the beater and its striking frequency. Empirical correlations are proposed and good agreements between experimental and predicted values were obtained since the standard deviation is lower than 20% for the whole dataset.

**Keywords**: Mixing time; soft elastic reactor; viscous fluid; modelling; crank/slider; impulse; momentum change.

## 1. Introduction

Chen et al.,[1] working on bio-inspired chemical engineering reactors (BioChE defined by Chen, 2016), recently introduced a new homogenization system referred to as a soft elastic reactor (SER) to the mixing community.[2-6]

This mixing system consists of a soft container that can achieve homogenization through vibrations of the tank wall (Fig. 1). With no agitator in contact with the agitated media, it offers advantages for many potential mixing applications, both at the laboratory and the industrial scale, as previously reported by Delaplace et al. (2018).[7] Two relevant applications of this mixing equipment in the field of chemical engineering are: (i) disposable containers, skipping sterilization and cleaning steps compared to traditional bioreactors used for microbial cultivation, and (ii) mixing operations involving highly corrosive media as any problem of corrosion of the agitator is eliminated in this case.

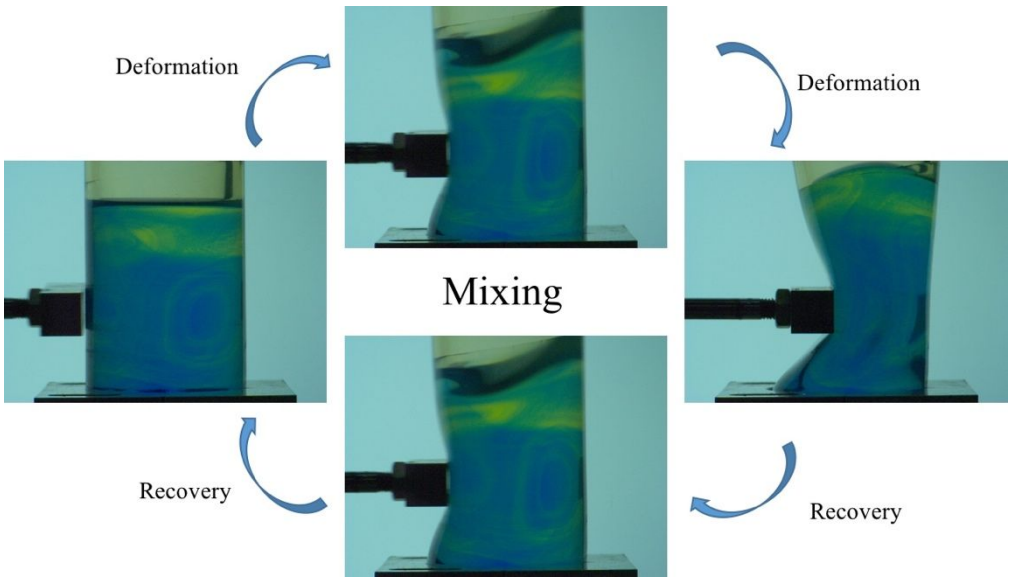


Figure 1. The mixing process of a soft elastic reactor showing cyclic deformation and recovery of the reactor wall. The tip of the piston of a slider crank device is shown here.

It should be noted that fluid homogenization induced by fluctuating external perturbations has attracted little attention until now in the mixing community. The current lack of experimental data on the parameters governing the homogenization course in such mixing equipment as well as the absence of predictive models describing the performance of such mixing systems are obstacles to be overcome to convince engineers to use this mixing system more extensively.

An interesting contribution was recently made in this field by Delaplace et al. (2018) using the dimensional analysis approach.[7] Specifically, three groups of dimensionless numbers were found to influence the mixing progress. In particular, these dimensionless numbers include: (i) those containing the variables responsible for wall vibrations (i.e., the maximum penetration depth, the height of the beater from the bottom of the tank, and the angular frequency of the beater); (ii) dimensionless numbers characterizing the deformation and recovery of the soft

elastic wall (i.e., the elastic properties of the material, wall thickness, clamp protocol); and (iii) dimensionless ratios defining the liquid properties contained in the tank and the liquid height.

This modeling effort has allowed us to define two dimensionless numbers: the mixing time $(\theta_m)$ and the Reynolds $(Re)$ number for this special type of mixing equipment:

$$\theta_m = f \cdot t_m \quad (1)$$

$$Re = \frac{\rho \cdot f \cdot T^2}{\mu} \quad (2)$$

In Eqs. (1) and (2), $t_m$ is the mixing time required to obtain the desired degree of homogeneity, whereas $\rho$ and $\mu$ are the density and viscosity, respectively, of the agitated Newtonian media to be homogenized. $f$, refers to the striking frequency of the beater, while $T$ is the container diameter.

More precisely, for a given tank containing a fixed liquid height and a given position of beater strikes on the outside wall of the reactor, Delaplace et al. (2018) reported that the mixing time number depends on four dimensionless numbers:[7]

$$\theta_m = F_1\left( Re, Ga, \frac{p}{T}, \frac{C_b}{T} \right) \quad (3)$$

where $Ga = \frac{g \cdot T^3 \rho^2}{\mu^2}$ is the Galilei number of the soft elastic reactor, whereas $\frac{p}{T}$ and $\frac{C_b}{T}$ are two geometrical ratios that describe the beater action and position. In Eq. (3), the Galilei number is an internal measurement (consisting of repeated physical quantities specific to the studied mixing system) that takes the effect of gravity on the free surface of the liquid into account. The Galilei impact is supposed to be significant when free surface of the liquid is no longer flat and vortex is capable of changing the mixing progress. $\frac{p}{T}$ is a ratio arising from the fact that different maximum penetration depths, $p$, could be set. Note that the maximum penetration depth $p$ with which the beater periodically deforms the soft elastic wall was measured by Delaplace et al.

(2018).[7] However, this value could also be deduced from the knowledge of the geometrical parameters of the crank/slider device (including the crank radius $R$, the rod length $L$ and the distance from the rod pin to the piston pin $l_1$) and of the distance separating the crankshaft center to the vertical tank wall ($d_{sw}$), as shown in Fig. 2.

$$p = d_{sw} - R - L - l_1 \quad (4)$$

$\frac{C_b}{T}$ is a ratio that takes the bottom clearance of the beater into account. Note that various distances between the horizontal axis that defines the beater course $C_b$ and the tank bottom could be used for our setup.

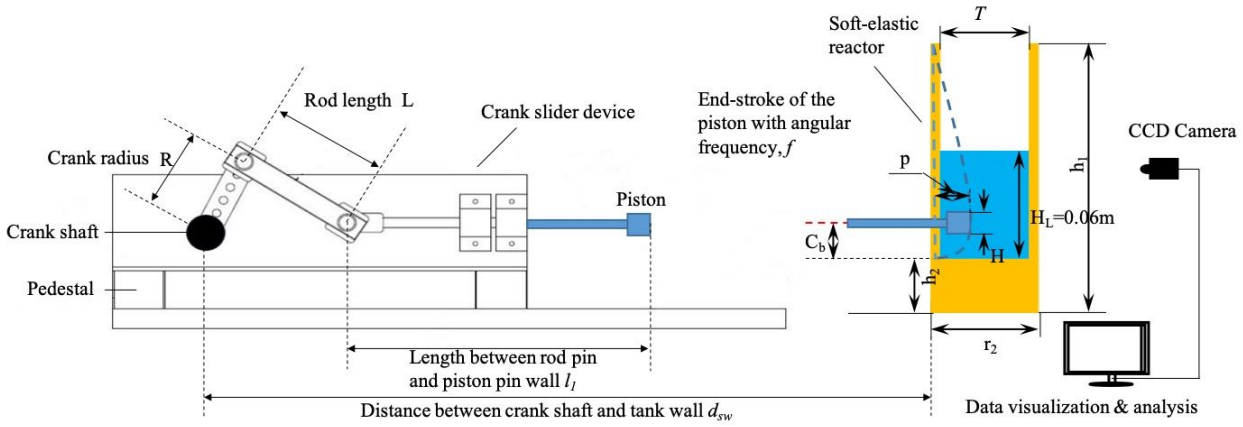


Figure 2. Sketch and geometrical parameters of the drive system (crank/slider device, left side) of the soft elastic reactor and of the digital image acquisition system (right).

Delaplace et al. (2018)[7] also carried out experimental measurements of mixing times by varying parameters $p$, $C_b$, $f$ and the viscosity of Newtonian fluids. Their study provides insights into the shape of the mixing curve and influential parameters.

Based on the experimental system's capabilities, the range of varying parameters was chosen to cover the largest flow range regimes in the container, i.e. from the laminar regime

(Re<3) to the turbulent mixing regime (Re>60). The main information collected from experimental data could be briefly summarized as follows:

- for the experimental range investigated, analysis of mixing time data shows that the SER mixing number mainly depends on Reynolds numbers, is slightly affected by $\left(\frac{C_b}{T}\right)$ and not influenced by the Galilei number value. Absence of free surface deformation was clearly noted by the authors for the operating conditions applied in this work and it is therefore expected that the Galilei number should be negligible for these experiments. Moreover, the authors suggest that the impact of $\left(\frac{C_b}{T}\right)$ on mixing time was expected to be weak since the ratio between tank diameter and liquid height $\frac{T}{H_L}$ is equal to 0.833 and, in this context, it could be assumed that wall deformation is strong enough to induce convection motion in the whole tank. This will not necessarily be the case if this ratio becomes higher.

- analysis of the form of the mixing curve for a given maximum penetration depth ratio (equal to a $\frac{p}{T}$ of 0.42) revealed that, under a laminar regime, a fixed number of strikes, $f \cdot t_m$, is necessary to obtain the anticipated homogeneity level. On the contrary, a drastic decrease in the number of strikes is reported when the transition regime is reached.

It can be observed that the number of strikes required to achieve the desired homogeneity level increases when $\frac{p}{T}$ decreases but the sigmoidal shape of the mixing curve remains similar, regardless of the fixed $\frac{p}{T}$ values. However, this increasing number of strikes required to reduce heterogeneity with decreasing $\frac{p}{T}$ values seems also to be significantly influenced by the flow regime (Reynolds number). This trend is not illogical from a physical point of view since the convection of liquid elements induced by the deformation of the soft elastic surface is supposed

to have a greater influence when the flow regime is laminar in comparison to transition and turbulent regime, the molecular diffusion being restricted in this case.

Finally, the authors emphasized that the S-shaped mixing curves of the SER are very similar to those obtained with traditional mixers like helical ribbon agitators used for homogenizing liquids. They mentioned that some analogies exist between mixing curves of classical mixing systems (for which an agitator performs one revolution around a vertically centered axis) and this soft elastic reactor. For a tank equipped with one central agitator, a fixed number of revolutions of the agitator should be completed in order to obtaine the targeted homogeneity level. Here, for the soft elastic reactor, a fixed number of strikes is necessary for obtaining the desired degree of homogeneity. In the two cases, the displacement of a tool (agitator inside the tank or beater outside the container) is responsible for the mixing progress.

The pioneering study of Delaplace et al. (2018) is the only one that includes a dimensional analysis on a soft elastic reactor, paving the way for the identification of the key dimensionless numbers that govern homogenization operations.[7] This approach also gave a first idea about controlling the mixing dynamics of liquids in a SER and allowed a comparison with homogenization mechanisms achieved by classical mixers.

Unfortunately, this preliminary “blind dimensional analysis” was not fully satisfactory. This approach can only provide limited insights into the physics governing the mixing time of the soft elastic reactor. Physical quantities such as impulse induced by the piston or change in momentum of the piston induced by the strike, which are considered to be the underlying parameters of the mixing process, did not appear in the model. Consequently, at this stage, it is difficult to determine how the maximum penetration depth of the beater and the angular frequency of the crank contribute to modifying the impulse or change in momentum provided by

the beater. Moreover, no empirical process relationship was proposed to correlate mixing time with the operating parameters (i.e., causal inlet variables).

To fill this gap, it was decided:

i) To make a dimensional analysis for a second time, introducing an intermediate variable with full physical meaning into the relevant list, i.e., impulse or change in momentum induced by the strike. This is not an easy task since analytical estimation of these intermediate physical quantities required analysis of the kinetic motion of the piston. Precisely, an expression of these physical quantities and their variations based on the knowledge of the inlet parameters of the crank mechanism (the angular frequency of the crank (in rev/s) and the distance separating the crankshaft center to the vertical tank wall (in meters)) should be theoretically established.

ii) To re-analyze the experimental data in this new $\pi$-space in order to propose predictive empirical correlations of mixing time that involve change in momentum or impulse.

## 2. Materials and Methods

### *2.1. Soft elastic reactor under investigation*

Figure 1 shows the deformation and the recovery of the container wall upon the beater strike. Figure 2 illustrates the three main parts constituting the SER: a transparent container with elastic walls, a slider crank device to deform periodically the wall by a piston tip, a camera which allows us to obtain digital images of mixing progress.

Figure 2 reports the geometrical parameters that are required to describe the container and the position of the beater. The total height, $h_1$, the external diameter, $r_2$, and the base height at the bottom, $h_2$, of the soft elastic tank were respectively 0.15 m, 0.06 m and 0.03 m. The height of the liquid inside the tank $H_L$ was 0.06 m. The internal diameter of the tank $T$ was 0.05 m. The bottom part of the container was 'clamped' to ensure a good fixature. The geometrical parameters of the crank/slider device are also included in Fig. 2. The crank radius $R$, the rod length $L$ and the distance from the rod pin to the piston pin $l_1$were 0.035 m, 0.14 m and 0.21 m, respectively. Note that the crank/slider device induces a displacement of the piston pin along the horizontal axis. In fact, the piston oscillates around the soft container wall. Depending on the angle between the crank and the horizontal axis, the abscissa of the piston on the horizontal axis varies. Consequently, for a fixed crank/slider device and a given distance between the crankshaft and the vertical wall of the container ($d_{sw}$), the maximum penetration depth $p$ varies.

*2.2. Mixing fluid*

The liquids to be homogeneized are Newtonian media with a viscosity (μ) varying from 0.0285 Pa·s to 1.187 Pa·s. Their density ($\rho$) was measured in between 1190 kg/m$^3$ and 1272 kg/m$^3$. These two liquid properties were considered at 25ºC, which corresponds to the bulk temperature of the fluid inside the tank.

*2.3. Mixing time measurements*

Mixing time was deduced by analyzing the color change in the fluid induced by a decolorization reaction. The injected acidic fluid has properties similar to the agitated basic media. Reliability and repeatability of the colorimetric diagnosis applied to a soft elastic reactor

has recently been achieved.[5] The mixing time was defined as the duration from the injection up to the time instant for which the degree of homogeneity becomes consistently higher than 90%. All details concerning the injection of the acidic liquid into the basic agitated media, decolorization monitoring, the definition of the degree of homogeneity and the determination of mixing time are the same as those given in previous publications by Delaplace et al. (2018) and will not be repeated here for the sake of brevity.[7] During mixing experiments, the maximum penetration depth $p = d_{sw} - R - L - l_1$, the bottom clearance, $C_b$, and the crank slider frequency, $f$, have been set from 0.015 to 0.025 m, 0.025 m, and 0.5 to 3.0 cycles/second, respectively.

*2.4. Impulse evaluation*

As shown in Eq. (5), the impulse is the integration of the transversal force of the piston (which corresponds to the *x*-component force exerted by the piston pin), $F_p(\theta)$ (Fig. 3) within the interval of time defined between the instant $t_c$ when the piston comes in contact with the soft container ($\theta = \theta_c$), and the instant $t_p$ at which the maximum penetration depth of the piston in the soft reactor ($\theta = \theta_p$) occurs.

$$I = \int_{t_c}^{t_p} F_p(\theta)\, dt \tag{5}$$

Consequently, evaluation of the impulse requires the analytical expression of $F_p(\theta)$ and the knowledge of the two instants of time, $t_c$ and $t_p$. The well-known rectangular method was used to approximate the definite integral that appears in Eq. (5).

The following assumptions were made: (i) the weights of the crank and the follower can be neglected; (ii) the slider crank mechanism is a totally frictionless system; and (iii) the crank rotates clockwise at a constant angular velocity, $\dot{\theta} = \omega$ (Fig. 3), and the x-component force

exerted by the slider $F_p$ can be theoretically obtained from the knowledge of the instantaneous acceleration of the piston, $Acc(\theta) = \left\|\frac{d^2\overrightarrow{OB}}{dt^2}\right\|$:

$$F_p(\theta) = m_{piston} \cdot \left\|\frac{d^2\overrightarrow{OB}}{dt^2}\right\| \quad (6)$$

In Eq. (6), $m_{piston}$ is the piston mass (i.e., 0.06093 kg in this study). Note that in Eq. (6), piston mass is sometimes replaced by a reciprocating mass, which corresponds to the piston mass, plus approximately 2/3 of the connecting rod mass. In this case, the piston mass was used.

It can be shown that the instantaneous acceleration, $\left\|\frac{d^2\overrightarrow{OB}}{dt^2}\right\| = \left\|\frac{d^2\overrightarrow{OM}}{dt^2}\right\|$, can be deduced by differentiating the displacement of the piston $\overrightarrow{OM}$ with respect to the crank angle $\theta$, which can be derived using simple trigonometry.

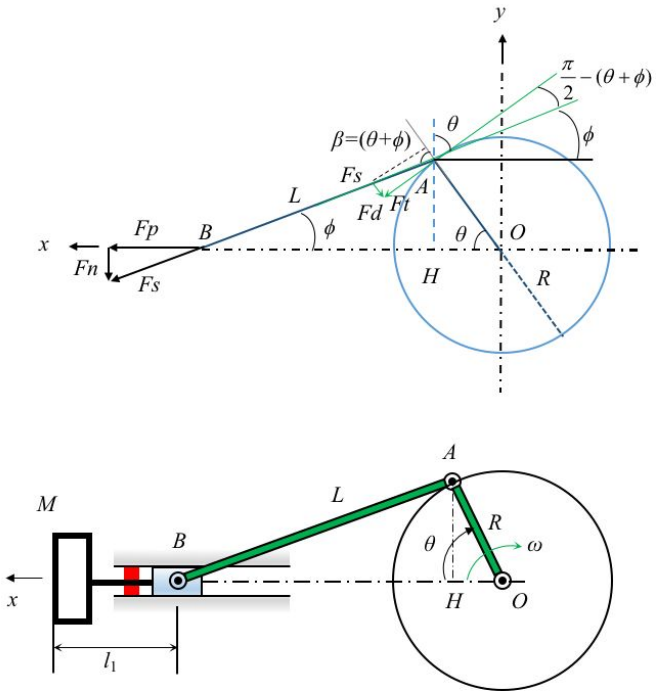


Figure 3. Kinetic motion of crank/slider device and forces induced by the crank mechanism.

Indeed, from Fig. 3, it can be observed that:

$$\overrightarrow{OM} = \overrightarrow{OA} + \overrightarrow{AB} + \overrightarrow{BM} \quad (7)$$

which becomes:

$$\overline{OM} = Rcos\theta + Lcos\emptyset + l_1 \quad (8)$$

On the basis of Fig. 3, it can be also established that:

$$HA = sin\emptyset \cdot L = R \cdot sin\theta \quad (9)$$

Consequently, $\emptyset = arcsin\left[\frac{R}{L} \cdot sin\theta\right]$ (10)

and

$$\cos\emptyset = cos\left(arcsin\left[\frac{R}{L} \cdot sin\theta\right]\right) = \left(1 - \left[\frac{R}{L} \cdot sin\theta\right]^2\right)^{1/2} \quad (11)$$

Introducing Eq. (11) into Eq. (8) gives Eq. (12):

$$\overline{OM} = Rcos\theta + L\left(1 - \left[\frac{R}{L} \cdot sin\theta\right]^2\right)^{1/2} + l_1 \quad (12)$$

Taking the derivative of Eq. (12) with respect to time gives:

$$V(\theta) = \left\|\frac{d\overrightarrow{OM}}{dt}\right\| = -R \cdot sin\theta \cdot \omega - \cdot L \cdot \left(1 - \left[\frac{R}{L} \cdot sin\theta\right]^2\right)^{-\frac{1}{2}} \left[\frac{R}{L}\right] \cdot sin\theta \cdot \omega \cdot cos\theta \cdot \left[\frac{R}{L}\right] \quad (13)$$

where $\dot{\theta} = \omega = 2 \cdot \pi \cdot f$ (14)

The derivative of Eq. (10) gives:

$$\frac{d\emptyset}{dt} = \left(1 - \left[\frac{R}{L} \cdot sin\theta\right]^2\right)^{-1/2} \cdot \omega \cdot cos\theta \cdot \left[\frac{R}{L}\right] = \omega \cdot \frac{R}{L} \cdot \left[\frac{cos\theta}{cos\emptyset}\right] \quad (15)$$

Combining Eq. (15) with Eq. (13) also gives:

$$V(\theta) = \left\|\frac{d\overrightarrow{OM}}{dt}\right\| = \left\|\frac{d\overrightarrow{OB}}{dt}\right\| = \quad -R \cdot sin\theta \cdot \left(\omega + \frac{d\emptyset}{dt}\right) \quad (16)$$

The derivative of Eq. (16) allows us to obtain the expression of piston acceleration (Eq. (17)). It can be shown that:

$$\left\|\frac{d^2\overrightarrow{OM}}{dt^2}\right\| = \left\|\frac{d^2\overrightarrow{OB}}{dt^2}\right\| = Acc(\theta) = -R\cdot\omega\cdot\cos\theta\cdot\left(\omega+\frac{d\emptyset}{dt}\right) - R\cdot sin\theta\cdot\left(\left(\frac{d^2\emptyset}{dt^2}\right)\right) \quad (17)$$

where $\frac{d^2\emptyset}{dt^2} = \frac{\left(-R\cdot\omega^2\cdot[sin\theta]\right) + L\cdot\left(\frac{d\emptyset}{dt}\right)^2\cdot sin\theta}{L\cdot cos\emptyset}$ (18)

is obtained by taking the derivative of Eq. (15).

*2.5. Change in momentum evaluation*

Momentum is the product of piston mass multiplied by its velocity. The change in momentum (denoted $m_{piston}\Delta V$) is the difference between the momentums evaluated at the instant $t_c$ at which the piston comes in contact with the soft container and at the instant of time $t_p$ at which the maximum penetration depth of the piston in the soft reactor occurs. For this last instant of time, the velocity of the piston becomes equal to zero. Consequently, the change in momentum can be rewritten as:

$$m_{piston}\Delta V = m_{piston}\cdot V(\theta=\theta_c) \quad (19)$$

In Eq. (19), $V(\theta=\theta_c)$ is the velocity of the piston evaluated at the angular position $\theta_c$ at which the piston comes in contact with the tank. The angular position $\theta_c$ at which the piston comes in contact with the tank depends on the fixed value of the maximum penetration depth *p*.

*Evaluation of the angular position $\theta_c$ at which the piston comes in contact with the tank*

The piston comes in contact with the tank when:

$$\overline{OM} = R + L + l_1 - p \quad (20)$$

Therefore, introducing Eq. (20) into Eq. (12), the crank angle $\theta_c$ at which the piston comes in contact with the tank could be obtained by rearranging Eq. (21):

$$R + L + l_1 - p = Rcos\theta_c + L\left(1 - \left[\frac{R}{L}\cdot sin\theta_c\right]^2\right)^{1/2} + l_1 \quad (21)$$

*Evaluation of the instant of time $t_c$ at which the piston comes in contact with the tank*

Consequently, the instant of time $t_c$ at which the piston comes in contact with the tank could also be determined:

$$t_c = \theta_c/\ \omega = \theta_c/(2 \cdot \pi \cdot f) \quad (22)$$

*Evaluation of the velocity at which the piston comes in contact with the tank* $(\theta = \theta_c)$

Knowledge of the crank angle $\theta_c$ at which the piston comes in contact with the tank allows us to evaluate the velocity of the piston when it is in contact with the soft reactor:

$$V(\theta = \theta_c)\ = -R \cdot sin\theta \cdot \omega - \cdot L \cdot \left(1 - \left[\frac{R}{L} \cdot sin\theta_c\right]^2\right)^{-1/2}\left[\frac{R}{L}\right] \cdot sin\theta_c \cdot \omega \cdot cos\theta_c \cdot \left[\frac{R}{L}\right] \quad (23)$$

*Evaluation of angular position $\theta_p$ at which the piston reaches the maximum penetration depth*

The piston reached the maximum penetration depth when:

$$\overline{OM} = R + L + l_1 \quad (24)$$

On the basis of Fig. 3, it could be observed that this piston tip position is achieved when:

$$\theta_p = 2\pi \quad (25)$$

For this angular position, the piston velocity, $V(\theta = \theta_p)$ becomes zero.

Consequently, the instant of time $t_p$ at which the piston *reaches the maximum penetration depth* could also be determined:

$$t_p = \theta_p/\ \omega = \theta_p/(2 \cdot \pi \cdot f) = 1/f \quad (26)$$

## 3. Results and Discussion

*3.1. Dimensional analysis of mixing time in SER with impulse or change in momentum introduced as intermediate variables*

Dimensional analysis is a powerful tool to investigate the link that exists between the inlet and outlet parameters of a system and to determine the mathematical correlations that describe the causal relationship. In a recent book, Delaplace et al. (2015) reviewed in detail how dimensionless numbers should be rigorously constructed.[8] The recommended guidelines for applying a dimensional analysis were strictly implemented here, taking mixing time measured in the container as the output and the operating parameters of the crank/slider device as the inlet of the studied system.

Figure 2. represents the soft elastic container hit by the beater of the crank slider device. Analysis of Fig. 2 clearly shows that the liquid homogenization in such a reactor is influenced by the following variables:

- geometrical parameters delimitating the flow domain. They include the container inner diameter, $T$, and the liquid height, $H_L$. Since a field of gravity exists at the free surface of the liquid, acceleration $g$ should not be omitted, although it is a constant in all experiments.

- material properties of the fluids in the SER. These agitated liquids are Newtonian fluids. Consequently, density ($\rho$) and viscosity ($\mu$) are intrinsic properties and constant in all the volume of the vessel. Note that the diffusion coefficient was not retained in the relevant list of parameters since it has been numerously and previously established that convection is preponderant for driving the mass transfer of such a system.

- process parameters, namely:

(i) the impulse $I$ or the change in momentum $m_{piston}\Delta V$, which are the underlying physical quantities that have a significant influence on the mixing of fluids inside the vessle;

(ii) the period $(1/f)$ of the collision between the beater and the container wall. $f$ is the angular frequency of the crank (in rev/s).

- parameters that describe the way the impulse or change in momentum is dissipated to the wall of the container and the definition of the recovery properties of the soft elastic reactor after deformation. Among them, we can include:

(i) the height and width of the beater (in m), $H$ and $w$, respectively which define the contact surface with which the beater transmits the impulsion or change in momentum;

(ii) the bottom clearance of the piston $C_b$ (i.e., the distance between the horizontal axis defining the beater course and the bottom of the tank) that defines the position at which the initial deformation is induced.

At the end of the of the maximum penetration depth, it is mandatory for the piston to retreat. Consequently, the deformed wall of the SER starts to recover (see Fig. 1). This step is driven by the elastic properties and thickness of the vertical wall and is expected to influence the mixing course inside the container. Hence, it is important to integrate in the relevant list of the dimensional analysis the physical quantities responsible for this recovery behaviour. In our work, the elastic modulus (also known as the Young's modulus $E$) of the container material, and some geometrical parameters that can characterize the SER behavior during recovery (e.g. height $h_1$, base height $h_2$, and outer diameter $r_2$ of the tank) have been listed.

Finally, depending on whether the impulse $I$ or the change in momentum $m_{piston}\Delta V$ is introduced into the relevant list, the SER homogenizing process can therefore be expressed by the relationship:

$$t_m = F_2(h_1, h_2, r_2, E, T, H_L, C_b, H, w, I, \rho, \mu, 1/f, g) \quad (27)$$

$$t_m = F_3(h_1, h_2, r_2, E, T, H_L, C_b, H, w, m_{piston}\Delta V, \rho, \mu, 1/f, g) \quad (28)$$

Choosing $(T, \rho, g)$ as the repeated physical variables, the corresponding dimensionless ratios associated with SER mixing time are:

$$\frac{t_m \cdot g^{1/2}}{T^{1/2}} = F_4\left(\frac{h_1}{T}, \frac{h_2}{T}, \frac{r_2}{T}, \frac{E.}{\rho \cdot T g}, \frac{H_L}{T}, \frac{C_b}{T}, \frac{H}{T}, \frac{w}{T}, \frac{I}{\rho.g^{1/2}T^{7/2}}, \left(\frac{g \cdot T^3 \rho^2}{\mu^2}\right), \pi_1 = \left(\frac{g^{1/2}}{T^{1/2}.f}\right)\right) \quad (29)$$

$$\frac{t_m \cdot g^{1/2}}{T^{1/2}} = F_5\left(\frac{h_1}{T}, \frac{h_2}{T}, \frac{r_2}{T}, \frac{E.}{\rho \cdot T g}, \frac{H_L}{T}, \frac{C_b}{T}, \frac{H}{T}, \frac{w}{T}, \frac{m_{piston}\Delta V}{\rho.g^{1/2}T^{7/2}}, \left(\frac{g \cdot T^3 \rho^2}{\mu^2}\right), \pi_1 = \left(\frac{g^{1/2}}{T^{1/2}.f}\right)\right) \quad (30)$$

In Eqs. (29) and (30), $\frac{t_m \cdot g^{1/2}}{T^{1/2}}$ is a dimensionless ratio that includes mixing time $t_m$. $\frac{I}{\rho.g^{1/2}T^{7/2}}$ and $\frac{m_{piston}\Delta V}{\rho.g^{1/2}T^{7/2}}$ are two dimensionless numbers that quantify the impulse or the change in momentum induced by the beater, respectively. These two numbers are different ways to express the intensity of the collision at which the piston strikes the containers and could be theoretically or experimentally estimated. These values of the two dimensionless numbers are governed by the geometrical parameters of the crank/slider device (the crank radius $R$, the rod length $L$ and the distance from the rod pin to the piston pin $l_1$), by the distance separating the crankshaft center $d_{sw}$to the vertical tank wall, and by the angular crank frequency $f$. Indeed, depending on these physical quantities, the maximum penetration depth, the velocity at which the piston comes in contact with the soft container, and the length of time of the collision will be different, as previously explained.

$\pi_1 = \left(\frac{g^{1/2}}{T^{1/2}.f}\right)$ is a dimensionless number that provides an internal measurement of the period of the clash. Consequently, the higher the angular crank frequency $f$ is, the shorter the time between two collisions will be, and the shorter $\pi_1 = \left(\frac{g^{1/2}}{T^{1/2}.f}\right)$will be.

In Eq. (30), $Ga = \frac{g \cdot T^3 \rho^2}{\mu^2}$ is the SER Galilei number, that provides an internal measure of how the viscosity of the fluid can influence the mixing process.

It was decided to make some re-arrangements and to replace $\pi_1$ with ${\pi_1}^{-2}$ in order to make a modified Froude number, ${\pi_1}^{-2} = Fr,$ appear. In this configuration, the Froude number,

$Fr = \frac{f^2 \cdot T}{g}$ , provides a measurement of beater frequency. Consequently, the higher the angular crank frequency is, the shorter the period of the collision, the higher the Froude number and the higher the number of strikes delivered by the piston during a given period of time will be.

As a result, another $\pi$ -space could be used to describe the SER mixing process :

$$\frac{t_m \cdot g^{1/2}}{T^{1/2}} = F_6\left(\frac{h_1}{T}, \frac{h_2}{T}, \frac{r_2}{T}, \frac{E.}{\rho \cdot T g}, \frac{H_L}{T}, \frac{C_b}{T}, \frac{H}{T}, \frac{w}{T}, \frac{I}{\rho . g^{1/2} T^{7/2}}, Fr, Ga\right) \quad (31)$$

$$\frac{t_m \cdot g^{1/2}}{T^{1/2}} = F_7\left(\frac{h_1}{T}, \frac{h_2}{T}, \frac{r_2}{T}, \frac{E.}{\rho \cdot T g}, \frac{H_L}{T}, \frac{C_b}{T}, \frac{H}{T}, \frac{w}{T}, \frac{m_{piston} \Delta V}{\rho . g^{1/2} T^{7/2}}, Fr, Ga\right) \quad (32)$$

As explained by Delaplace et al. (2015) and White (2011), the choice of scaling variables and their recombinations is up to the users.[8,9] The choice will not affect the dimensional analysis, but only the form of its presentation.

In the section above, the scaling of Eqs. (27) and (28) was performed by introducing ($T$, $\rho$, $g$) as repeated variables instead of using another basis that could be used for scaling such as ($T$, $\rho$, $f$). This choice was made so that the period ($1/f$) of the beater strike appears only in one causal dimensionless number (in this case, $Fr = \frac{f^2 \cdot T}{g}$) and, consequently, isolate the influence of the beater frequency on the output (in our case, $\frac{t_m \cdot g^{1/2}}{T^{1/2}}$).

However, as in Delaplace et al. (2018), it is also possible to make some recombinations again from Eqs. (27) and (28) in order to give rise to different configurations (Eqs. (33) to (36)) containing other dimensionless numbers such as $f \cdot t_m$ (instead of $\frac{t_m \cdot g^{1/2}}{T^{1/2}}$) or Reynolds numbers, $Re = \frac{\rho \cdot f \cdot T^2}{\mu}$ (instead of $Fr = \frac{f^2 \cdot T}{g}$) for which more physical significance could be intuitively captured and/or more commonly adopted in the mixing community.[7]

$f \cdot t_m$ is obtained by multiplying $\frac{t_m \cdot g^{1/2}}{T^{1/2}}$ by $(Fr)^{1/2}$, whereas the Reynolds number is derived from the recombination $(Ga \cdot Fr)^{1/2}$.

In this case, among the multiple possibilities, Eqs. (31) and (32) could become:

$$\frac{t_m \cdot g^{1/2}}{T^{1/2}} = F_{12}\left(\frac{h_1}{T}, \frac{h_2}{T}, \frac{r_{2,}}{T}, \frac{E.}{\rho \cdot Tg}, \frac{H_L}{T}, \frac{C_b}{T}, \frac{H}{T}, \frac{w}{T}, \frac{I}{\rho.g^{1/2}T^{7/2}}, Fr, Re\right) \quad (33)$$

$$\frac{t_m \cdot g^{1/2}}{T^{1/2}} = F_{13}\left(\frac{h_1}{T}, \frac{h_2}{T}, \frac{r_{2,}}{T}, \frac{E.}{\rho \cdot Tg}, \frac{H_L}{T}, \frac{C_b}{T}, \frac{H}{T}, \frac{w}{T}, \frac{m_{piston}\Delta V}{\rho.g^{1/2}T^{7/2}}, Fr,\ Re\right) \quad (34)$$

$$f.t_m = F_8\left(\frac{h_1}{T}, \frac{h_2}{T}, \frac{r_{2,}}{T}, \frac{E.}{\rho \cdot Tg}, \frac{H_L}{T}, \frac{C_b}{T}, \frac{H}{T}, \frac{w}{T}, \frac{I}{\rho.g^{1/2}T^{7/2}}, Fr, Ga\right) \quad (35)$$

$$f.t_m = F_9\left(\frac{h_1}{T}, \frac{h_2}{T}, \frac{r_{2,}}{T}, \frac{E.}{\rho \cdot Tg}, \frac{H_L}{T}, \frac{C_b}{T}, \frac{H}{T}, \frac{w}{T}, \frac{m_{piston}\Delta V}{\rho.g^{1/2}T^{7/2}}, Fr, Ga\right) \quad (36)$$

$$f.t_m = F_{10}\left(\frac{h_1}{T}, \frac{h_2}{T}, \frac{r_{2,}}{T}, \frac{E.}{\rho \cdot Tg}, \frac{H_L}{T}, \frac{C_b}{T}, \frac{H}{T}, \frac{w}{T}, \frac{I}{\rho.g^{1/2}T^{7/2}}, Fr, Re\right) \quad (37)$$

$$f.t_m = F_{11}\left(\frac{h_1}{T}, \frac{h_2}{T}, \frac{r_{2,}}{T}, \frac{E.}{\rho \cdot Tg}, \frac{H_L}{T}, \frac{C_b}{T}, \frac{H}{T}, \frac{w}{T}, \frac{m_{piston}\Delta V}{\rho.g^{1/2}T^{7/2}}, Fr,\ Re\right) \quad (38)$$

When a given crank/slider device placed at a given bottom clearance is used to beat a given soft container filled with given viscous fluids at a constant liquid height, some geometrical ratios become fixed. Consequently, their effect on dimensionless mixing time could not be evaluated and the configurations should be reduced. In this case, Eqs. (31) and (38) become Eqs. (39) and (46).

$$f \cdot t_m = F_{14}\left(\frac{I}{\rho.g^{1/2}T^{7/2}}, Fr, Ga\right) \quad (39)$$

$$f \cdot t_m = F_{15}\left(\frac{m_{piston}\Delta V}{\rho.g^{1/2}T^{7/2}}, Fr, Ga\right) \quad (40)$$

$$f \cdot t_m = F_{16}\left(\frac{I}{\rho.g^{1/2}T^{7/2}}, Fr,\ Re\right) \quad (41)$$

$$f \cdot t_m = F_{17}\left(\frac{m_{piston}\Delta V}{\rho.g^{1/2}T^{7/2}}, Fr, Re\right) \quad (42)$$

$$\frac{t_m \cdot g^{1/2}}{T^{1/2}} = F_{18}\left(\frac{I}{\rho.g^{1/2}T^{7/2}}, Fr, Re\right) \quad (43)$$

$$\frac{t_m \cdot g^{1/2}}{T^{1/2}} = F_{19}\left(\frac{m_{piston}\Delta V}{\rho.g^{1/2}T^{7/2}}, Fr,\ Re\right) \quad (44)$$

$$\frac{t_m \cdot g^{1/2}}{T^{1/2}} = F_{20}\left(\frac{I}{\rho.g^{1/2}T^{7/2}}, Fr, Ga\right) \quad (45)$$

$$\frac{t_m \cdot g^{1/2}}{T^{1/2}} = F_{21}\left(\frac{m_{piston}\Delta V}{\rho.g^{1/2}T^{7/2}}, Fr, Ga\right) \quad (46)$$

Note that when the physical properties of the agitated fluid (density and viscosity) are also maintained unchanged for a given mixing equipment, the Galilei number also becomes constant and the configuration is reduced as much as possible. Equations (39), (40), (45) and (46) become:

$$f \cdot t_m = F_{22}\left(\frac{I}{\rho.g^{1/2}T^{7/2}}, Fr\right) \quad (47)$$

$$f \cdot t_m = F_{23}\left(\frac{m_{piston}\Delta V}{\rho.g^{1/2}T^{7/2}}, Fr\right) \quad (48)$$

$$\frac{t_m \cdot g^{1/2}}{T^{1/2}} = F_{24}\left(\frac{I}{\rho.g^{1/2}T^{7/2}}, Fr\right) \quad (49)$$

$$\frac{t_m \cdot g^{1/2}}{T^{1/2}} = F_{25}\left(\frac{m_{piston}\Delta V}{\rho.g^{1/2}T^{7/2}}, Fr\right) \quad (50)$$

The reduced $\pi$-spaces that appear in Eqs. (39) to (50) will be used later to represent and to interpret the SER mixing time data measured for different operating conditions.

### *3.2. Homogenization experiments and computational values of dimensionless numbers*

SER mixing experiments were carried out using different Newtonian fluids placed in a soft elastic container with a fixed liquid height (see Materials and Methods). The measured mixing times are given in Table S1. For these trials, the bottom clearance position of the piston was maintained constant and equal to 0.025 m. Crank angular frequency and maximum penetration depth *p* (by adjusting the distance separating the crankshaft center to the vertical tank wall $d_{sw}$) were adapted accordingly.

In Table S1, mixing experiments are sorted into two groups: (i) the ones obtained at a fixed value of Galilei number (trials #1 to #15), involving a fluid with constant density

(1263 kg m$^{-3}$) and Newtonian viscosity (1.25 Pa·s); and (ii) those obtained for varying values of Galilei number (trials #16 to #36), for which fluids density and Newtonian viscosity range from 1190 kg/m$^3$ to 1272 kg/m$^3$ and from 0.0285 Pa·s to 1.187 Pa·s, respectively.

At a whole, 108 experiments (36 experiments × 3 times) were performed to determine mixing times, but note that Table S1 only presents the average mixing time measured for each set of experimental conditions. The average standard deviation between repeated experiments for the 36 experiments was 10.4%.

Estimation of dimensional output parameters $\theta_c$, $t_c$, $V(\theta = \theta_c)$, $t_p$ and $I$ for the various imposed maximum penetration depths $p$ and angular frequencies $f$ (trials #1 to #36) are given in Table S2. The computed value of dimensionless numbers for the different mixing runs are given in Table S1.

Analysis of Table S2 shows us that the impulse dimensionless number and the change in momentum dimensionless number are equal. This result was expected since the impulse describes the change in momentum of the soft elastic reactor, and the estimation of these two intermediate physical quantities can be derived from a similar analysis (namely, the kinetic motion of the piston). The only difference between the estimation of these two physical quantities is that the change in momentum required less assumptions (assuming no loss of forces during the transmission).

For the sake of brevity, only $\pi$-spaces involving dimensionless impulses (given in Eqs. (39), (41), (43), (45), (47), (49) and (51)) were considered to discuss the SER mixing time data in the following.

*3.3. Influence of frequency and impulse on the internal measure of mixing time for fixed agitated media*

The evolution of the dimensionless SER mixing time based on the reduced configuration presented in Eq. (49) is represented in Fig. 4. The value of the Galilei number for this set of experiments was fixed (trials #1 to #15) and is equal to 1252. Since the Galilei number is fixed, the effect of the viscosity of the fluid in the container on mixing time are assumed to be constant and could not be interpreted (see Eq. (49)). Each symbol represents one mixing time experiment. For each symbol, the value of the impulse dimensionless number, $\frac{I}{\rho.g^{1/2}T^{7/2}}$ for which the mixing experiment was conducted is given in the legend. It should be recalled that each couple $(p,f)$ (representing maximum penetration depth and beater frequency), which are the commands of the mixing process, leads to one impulse value. The three different colors used for the symbols are visual guides for the three imposed maximum penetration depths. Red, orange and green are respectively for the maximum penetration depths of 0.015 m, 0.02 m, and 0.025 m.

Figure 4 plots the evolution of $(\frac{t_m \cdot g^{1/2}}{T^{1/2}})$ vs. $Fr$. As previously explained, the Froude number, $Fr = \left(\frac{f^2 \cdot T}{g}\right)$ is an internal measure of the beater frequency, and $(\frac{t_m \cdot g^{1/2}}{T^{1/2}})$ represents an internal measurement of the dimensionless mixing time.

Figure 4 reveals that both the beater frequency and the impulse values strongly affect the dimensionless mixing time number.

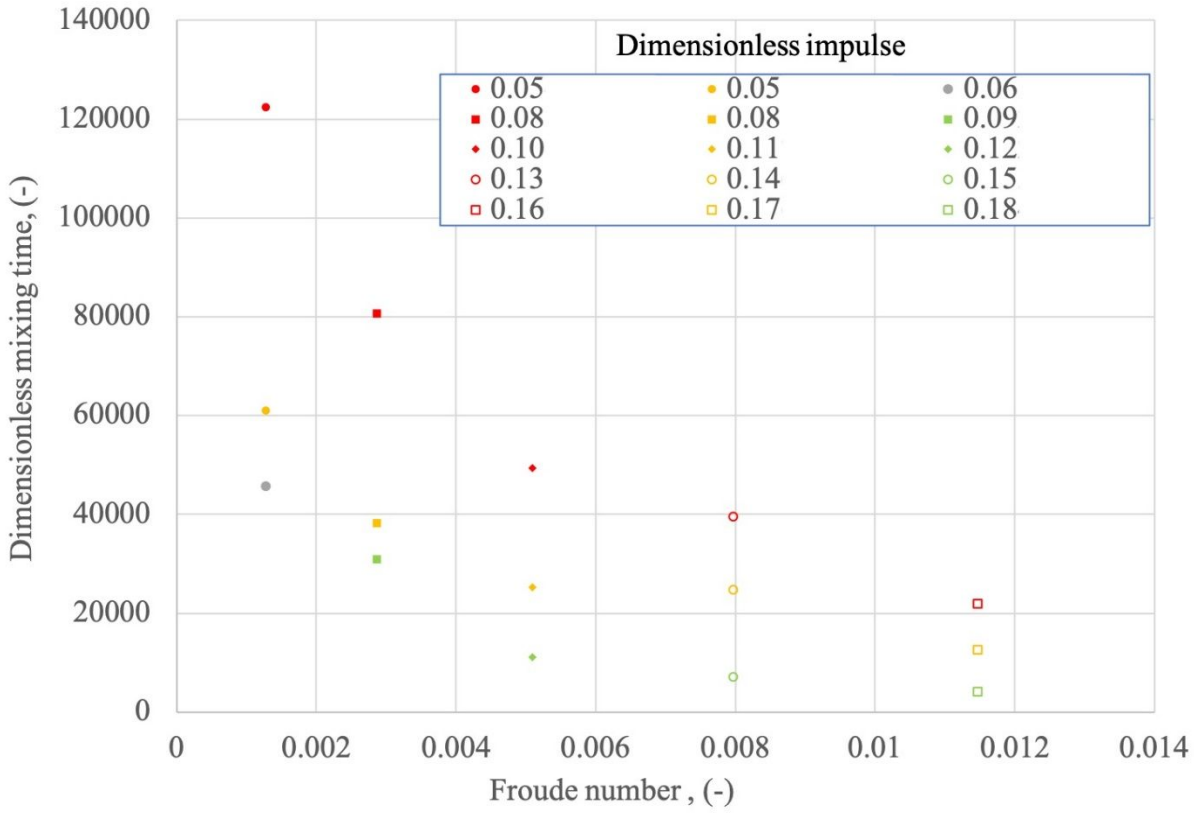


*Figure 4. Evolution of dimensionless mixing time for the soft elastic reactor* $\frac{t_m \cdot g^{1/2}}{T^{1/2}}$ *as a function of the modified Froude number* $Fr = \left(\frac{f^2 \cdot T}{g}\right)$.

At a given Froude number (beater frequency), a drastic decrease of dimensionless mixing time is observed for a small increase in the dimensionless impulse number. It can be concluded that for a fixed beater frequency, the greater the impulse is, the faster the desired degree of homogeneity will be obtained. It can also be observed that the decrease in mixing time with the increase in impulse is more pronounced when the beater frequency is low. For the range of Froude numbers investigated, it is clear that the beater frequency has less impact on dimensionless mixing time than an increase in impulse. These data describing the influence of impulse and frequency of collision on mixing time data are consistent with the expected physical trends.

Figure 5 is another representation of the evolution of the dimensionless SER mixing time, this time based on the reduced configuration of Eq. (47). In this figure, the number of strikes needed to reach complete homogenization, $f \cdot t_m$, is plotted on the ordinate axis.

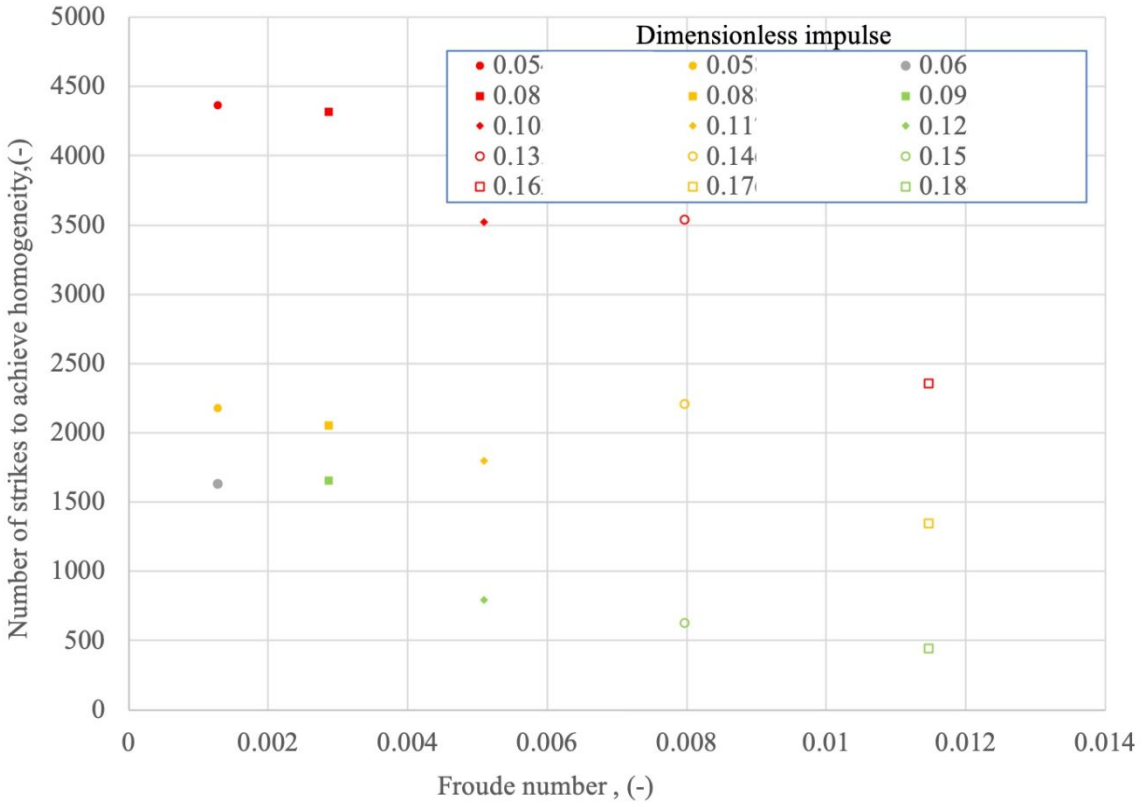


*Figure 5. Number of strikes of the piston required to achieve the desired level of homogeneity, $f \cdot t_m$, as a function of the modified Froude number, $Fr = \left(\frac{f^2 \cdot T}{g}\right)$.*

Figure 5 clearly shows that the number of strikes needed to reach complete homogenization in the SER is markedly influenced by the Froude number (beater frequency) and the impulse dimensionless values. For the range of Froude numbers and impulse dimensionless values considered, it appears that the impulse dimensionless number and the Froude number should be maximal in order to minimize the number of strikes.

To better quantify the effect of the impulse and frequency on the mixing process in the soft elastic reactor, it was decided in the next section to determine whether or not a predictive empirical correlation could be established. The number of strikes for achieving homogeneity was taken as the target variable.

*3.4. Correlation for predicting the number of strikes needed for reaching homogeneity*

The mixing process (and, consequently, the number of strikes needed for reaching a given homogeneity level) is assumed to be impacted by the viscosity of liquids in the container. As a consequence, an internal measurement appears in the dimensionless configuration to take the influence of viscosity (either the Galilei number in Eq. (39) or the Reynolds number in Eq. (41)) into account. However, we can observe that if mixing experiments are performed in a given soft reactor with a fixed fluid, the Galilei number becomes constant. As previously mentioned, this situation is interesting since the number of strikes becomes only a function of the impulse number and the Froude number, facilitating the determination of a mathematical equation for the process relationship. Therefore, in a first step, only experimental data obtained at a fixed Galilei number (Ga= 1252) were retained (trials #1 to #16) to identify the process relationship:

The following simple relationship could be proposed:

$$f \cdot t_m = A'\left(\frac{I}{\rho.g^{\frac{1}{2}}T^{\frac{7}{2}}}\right) + B' \quad (51)$$

where $A'$ and $B'$ are two power law functions of the Froude number:

$$A' = -6766.9\ Fr^{-1.114} \quad (52)$$

$$B' = 11077\ Fr^{-0.632} \quad (53)$$

Equation (51) is validated for:

$$1.27\ 10^{-3} < Fr < 1.15\ 10^{-2}; \qquad 6.14\ 10^{-2} < \left( \frac{I}{\rho . g^{\frac{1}{2}} T^{\frac{7}{2}}} \right) < 1.62\ 10^{-1};\ \text{Ga= 1252}$$

For a fixed Galilei number (Ga= 1252), the agreement between experimental and predicted data is good, as can be seen in Fig. 6.

For higher values of the Galilei number (ranging from 1252 to 3227657 from trials #17 to #32), it can be observed (Fig. 6) that predictive correlation progressively deviates from experimental values, leading to considerable scatters up to Galilei number values greater than 2200.

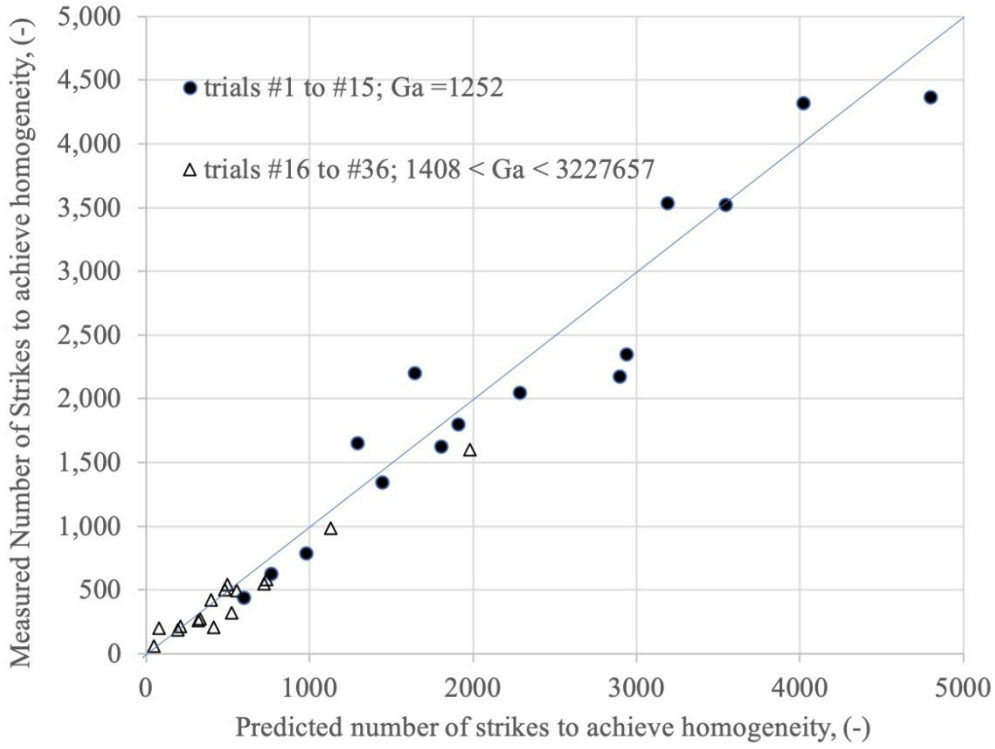


*Figure 6. Comparison between experimental and predicted values of the number of strikes needed for reaching homogeneity in the soft elastic reactor based on Eqs. (51) to (53).*

In order to go further and to find a predictive correlation that could be validated for the different fluids within the container of the soft elastic reactor, fitting with the help of a symbolic regression program (Eureqa) was attempted. All the experimental data were considered, taking

the number of strikes as outcome variables. $\pi$-spaces appearing in Eq. (41) were chosen to correlate the results since Reynolds and Froude numbers are more commonly adopted in the mixing community to describe viscosity and liquid-free surface deformation influences on the mixing process.

As was previously mentioned, a symbolic regression program could be very helpful to identify process relationships.[10,11] Since a sigmoid shape is expected for the evolution of the number of strikes as a function of Reynolds number for a given penetration depth ratio,[7] the corresponding mathematical model was looking forward in priority.

Thus, an empirical correlation describing the evolution of the number of strikes needed for reaching homogenization as a function of the Reynolds number and impulse number can be obtained. The mathematical equation of this correlation is given below:

$$\Theta_m = f \cdot t_m = \frac{\left(D\left(\frac{I}{\rho.g^{\frac{1}{2}}T^{\frac{7}{2}}}\right)^{-11.697} + E + 5.577\right)}{\left(1 + 0.569.Re^{-0.193}\right)^{-12.106}} - 5.577 \quad (54)$$

$$D = +20642.9\, Fr^{6.172} \quad (55)$$

$$E = -135.4\, Fr^{0.699} \quad (56)$$

Equation (54) is validated for:

$$1.3 < Re < 193; \qquad 1.27.10^{-3} < Fr < 4.59.10^{-2}; \qquad 6.14\,10^{-2} < \left(\frac{I}{\rho.g^{\frac{1}{2}}T^{\frac{7}{2}}}\right) < 3.66\,10^{-1}$$

Figure 7 shows that good agreement is observed for the whole set of data (the correlation coefficient is equal to 0.977). The standard deviation between experimental data and predicted values is equal to 21%. One difficulty here is to predict the number of strikes required for mixing processes that take place in transition and turbulent regimes since the decrease in the number of

strikes is very significant beyond the laminar regime and little experimental data is available to precisely identify the shape of the curve in these cases.

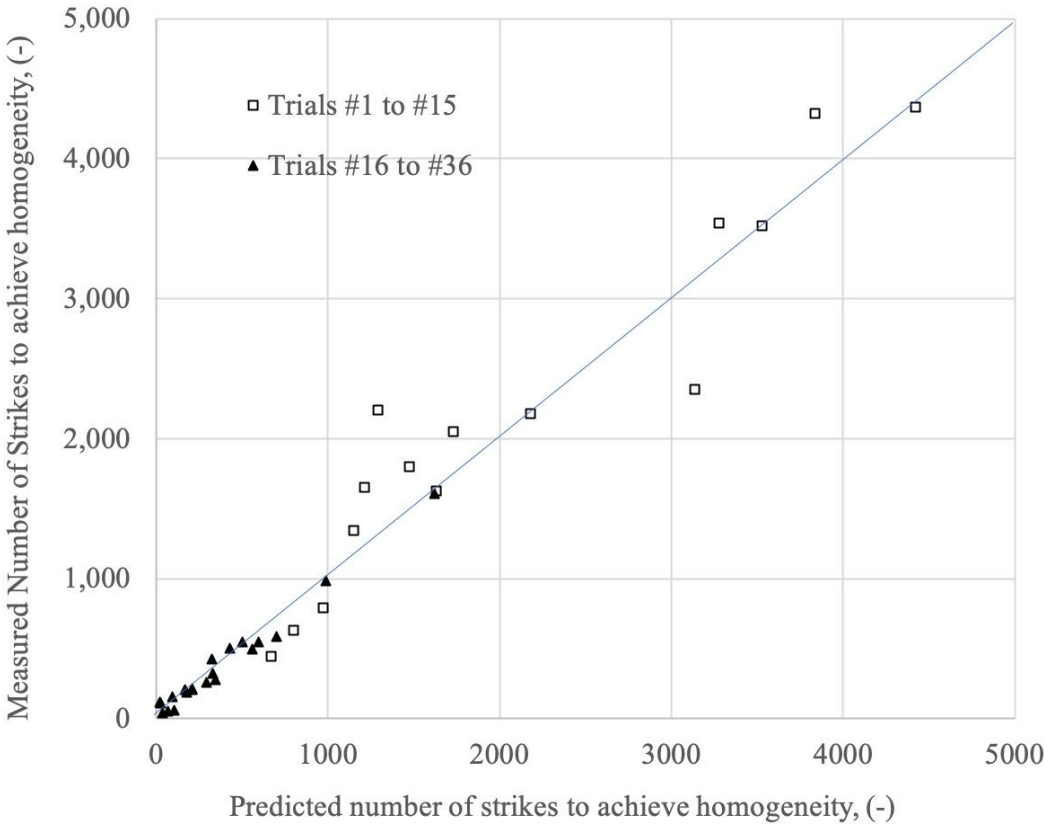


Figure 7. Predicted and experimental values for the number of strikes needed for reaching homogeneity. Experimental data are those given in Table S1.

## 4. Conclusion

In this study, mechanistic models linking the inlet parameters of the crank/slider device responsible for the tank wall vibrations to the mixing times were established for the soft elastic reactor. The mechanistic models are based on dimensional analysis and involve intermediate parameters with strong physical significance such as impulse and change in momentum. These intermediate quantities are derived from theoretical considerations. They are introduced in the

relevant list to take the intensity of mechanical sollicitation induced by the beater into account. Several $\pi$ -spaces were established to represent the SER mixing process, involving these intermediate quantities.

The experimental results showed that the number of strikes needed to reach a given degree of homogeneity is influenced by the Reynolds number, the impulse dimensionless number and the frequency of strikes. Finally, predictive correlations were obtained that covered various flow regimes, with a standard deviation within 20%.

**Notation**

| | |
|---|---|
| $C_b$ | Bottom clearance of the SER beater, m |
| $E$ | Young's modulus of the elastic material composing the SER wall, Pa |
| $f$ | Crank angular frequency and strike frequency, $s^{-1}$ |
| $Fr$ | SER Froude number (Eq. (31)) |
| $Ga$ | SER Galilei number (Eq. (3)) |
| $H$ | Beater height, m |
| $H_L$ | Liquid height in the tank, m |
| $h_1$ | SER tank height, m |
| $h_2$ | SER base height, m |
| $\frac{I}{\rho.g^{1/2}T^{7/2}}$ | SER impulse number (Eq. (29)) |
| $p$ | Maximum penetration depth, m |
| $Re$ | SER Reynolds number (Eq. (2)) |
| $R$ | Crank radius, m |
| $L$ | Rod length, m |

| | |
|---|---|
| $l_1$ | Distance from the rod pin to the piston pin, m |
| $t$ | Time, s |
| $t_m$ | SER mixing time, s |
| $T$ | Inner diameter of the vessel, m |
| $\frac{m_{piston}\Delta V}{\rho . g^{1/2} T^{7/2}}$ | Dimensionless number quantifying the change in momentum |

*Greek letters*

| | |
|---|---|
| $\mu$ | Newtonian viscosity, Pa·s |
| $\rho$ | Liquid density, kg $m^{-3}$ |

**Acknowledgements**

The authors deeply thank the National Key R&D Program of China (International S&T Cooperation Program, ISTCP, 2016YFE0101200), the National Natural Science Foundation of China (21676172, 21978184), the Natural Science Foundation of Jiangsu Province (BK20170062), and the "Priority Academic Program Development (PAPD) of Jiangsu Higher Education Institutions" for their financial support. Jie Xiao also acknowledges the "Jiangsu Innovation and Entrepreneurship (ShuangChuang) Program" and the "Jiangsu Specially-Appointed Professors Program".

**References**

(1) Chen, X. D. Scoping Biology-Inspired Chemical Engineering. *Chin. J. Chem. Eng.* **2016**, *24*, 1-8.

(2) Chen, X. D.; Liu, M. Material preparation and procedures for making a soft elastic reactor and the methods for mixing in this reactor. Patent CN104841299A, 2015.

(3) Liu, M.; Xiao, J.; Chen, X. D. A Soft-Elastic Reactor Inspired by the Animal Upper Digestion Tract. *Chem. Eng. Technol.* **2018**, *41*, 1051-1056.

(4) Liu, M. H.; Zou, C.; Xiao, J.; Chen, X. D. Soft-Elastic Bionic Reactor. *CIESC J.* **2018**, *69*, 414-422.

(5) Xiao, J.; Zou, C.; Liu, M.; Zhang, G.; Delaplace, G.; Jeantet, R.; Chen, X. D. Mixing in A Soft-Elastic Reactor (SER) Characterized Using An RGB Based Image Analysis Method. *Chem. Eng. Sci.* **2018**, *181*, 272-285.

(6) Zhang, G.; Liu, M.; Zou, C.; Xiao, J.; Chen, X. D. Enhancement of Liquid Mixing in A Soft-Elastic Reactor based on Bionics with An Elastic Rod. *Chem. Ind. Eng. Prog.* **2019**, *38*, 826-833.

(7) Delaplace, G.; Gu, Y.; Liu, M.; Jeantet, R.; Xiao, J.; Chen, X. D. Homogenization of Liquids Inside A New Soft Elastic Reactor: Revealing Mixing Behavior Through Dimensional Analysis. *Chem. Eng. Sci.* **2018**, *192*, 1071-1080.

(8) Delaplace, G.; Loubiere, K.; Ducept, F.; Jeantet, R. *Dimensional Analysis of Food Processes*; ISTE Press – Elsevier, 2015.

(9) White, F. M. *Fluid Mechanics* (*McGraw-Hill Series in Mechanical Engineering*); McGraw-Hill Publishing Co., 2011.

(10) Stoutemyer, D. R. Dimensional Analysis, Using Computer Symbolic Mathematics. *J. Comput. Phys.* **1977**, *24*, 141–149.

(11) Stoutemyer, D. R. Can the Eureqa Symbolic Regression Program, Computer Algebra, and Numerical Analysis Help Each Other? *Notices of the American Mathematical Society* **2013**, *60*, 713-724.

**Supporting Information**

This information is available free of charge via the Internet at http: //pubs.acs.org.

Two tables are supplied as supporting information.

Table S1. Mixing time obtained when homogenizing a given fluid (μ, $\rho$) in the soft elastic reactor and computed value of dimensionless numbers for the different trials (#1 to #36)

Table S2. Estimation of output parameters $\theta_c$, $t_c$, $V(\theta = \theta_c)$, $t_p$ and $I$ for the cases with different maximum penetration depths $p$ and angular frequencies $f$ (trials #1 to #36)

## TOC GRAPHIC

## For Table of Contents Only